

[Home](#) [Search](#) [Collections](#) [Journals](#) [About](#) [Contact us](#) [My IOPscience](#)

Ab *initio* parameterisation of the 14 band k·p Hamiltonian: Zincblende study

This content has been downloaded from IOPscience. Please scroll down to see the full text.

2014 J. Phys.: Conf. Ser. 526 012004

(<http://iopscience.iop.org/1742-6596/526/1/012004>)

View [the table of contents for this issue](#), or go to the [journal homepage](#) for more

Download details:

IP Address: 79.70.242.31

This content was downloaded on 01/04/2016 at 21:56

Please note that [terms and conditions apply](#).

Ab initio parameterisation of the 14 band $\mathbf{k}\cdot\mathbf{p}$ Hamiltonian: Zincblende study

Mark Lundie and Stanko Tomic

Joule Physics Laboratory, University of Salford, UK

E-mail: s.tomic@salford.ac.uk

Abstract.

Despite continued and rapid progress in high performance computing, atomistic level device modelling is still largely out of reach, necessitating the use of quantum mechanical continuum methods, including $\mathbf{k}\cdot\mathbf{p}$ perturbation theory. The effective use of such methods requires reliable parameterisation, often obtained from experiment and *ab initio* calculations. A major limitation of this, the systematic tendency of *ab initio* density functional theory to underestimate semiconducting material energy band gaps and related properties, can be greatly improved upon by the inclusion of exact exchange, calculated within the Hartree-Fock formalism. We demonstrate that the 14 band $\mathbf{k}\cdot\mathbf{p}$ Hamiltonian can be effectively parameterised using this method, at greatly reduced cost in comparison to GW methods.

1. Introduction

The modelling of semiconductor devices typically requires multiscale methods, whereupon calculations made at fundamental levels of theory are used to feed more approximate, but critically less computationally expensive, methods. *Ab initio* density functional theory (DFT) is commonly used for atomistic level calculations, which are then used to parameterise tight-binding (TB), empirical pseudopotential (EPM), or multiband $\mathbf{k}\cdot\mathbf{p}$ Hamiltonians [1]. Kohn-Sham DFT, however, does not yield the real band structure of semiconductors. Although a good approximation, the energy band gaps are systematically underestimated in this class of materials.

Many body perturbation theory, typically Green's function methods, can be used to more accurately predict the band gaps [2], but at considerable computational expense. An efficient and reasonably accurate alternative is the use of hybrid functionals [3, 4], which incorporate into the DFT exchange-correlation energy either a screened long range Coulomb term or a fraction of exact exchange calculated from Hartree-Fock theory using the Kohn-Sham orbitals.

Using this method, we calculate the necessary energy band gaps, dipole matrix elements, and effective masses at characteristic points in the first irreducible Brillouin zone (IBZ), i.e. at Γ point, to parameterise the 8 and 14 band $\mathbf{k}\cdot\mathbf{p}$ Hamiltonians. Although the 8 band $\mathbf{k}\cdot\mathbf{p}$ Hamiltonian, which has C_{4v} symmetry, is popular and widely used, it overlooks the correct C_{2v} atomistic symmetry of the zincblende (ZB) lattice [5]. In order to restore the correct symmetry it is necessary to implement the 14 band model, including couplings induced by the second conduction band (labelled as Γ_{5c} in fig. 1) stemming from p -bonding states of atoms in the ZB lattice [5]. We compare both to the DFT band structures in demonstration of this. We further



show the importance of non-locality in hybrid DFT calculations to the accurate prediction of band parameters.

2. Methodology

All DFT calculations are performed using the CRYSTAL [6, 7] code, which implements localised basis sets of Gaussian type orbitals (GTOs). The calculation of exact exchange is very efficient using this basis. The hybrid PBE0 [8] and B3LYP [9] exchange correlation functionals are used, the former incorporating 25% of exact exchange energy to the latter's 20%. The IBZ of the ZB lattice unit cell is sampled using the Monkhorst-Pack scheme [10], with shrinking factors $16 \times 16 \times 16$. Dipole matrix elements \mathbf{p}_{ij} are calculated from Bloch functions, $u_{\mathbf{k}i}(\mathbf{r})$, such that:

$$-i \frac{\hbar}{m_0} \mathbf{p}_{ij} = [E_i - E_j] \int d\mathbf{r} u_{\mathbf{k}i}^*(\mathbf{r}) \hat{\mathbf{r}} u_{\mathbf{k}j}(\mathbf{r}). \quad (1)$$

From the dipole matrix elements, Eq. 1, the Kane energies are calculated as follows:

$$E_P = \frac{2}{m_0} |\langle u_{c,0} | \hat{\mathbf{p}} | u_{v,0} \rangle|^2. \quad (2)$$

The *kppw* code [11], parameterised with the *ab initio* data, is used for all $\mathbf{k} \cdot \mathbf{p}$ calculations.

3. Results and discussion

Table 1 contains all the relevant parameters required for the parametrisation of unstrained 8 and 14 band $\mathbf{k} \cdot \mathbf{p}$ Hamiltonians for GaAs and CdSe, two common semiconductors that crystallise in the ZB structure.

Direction	Parameter	GaAs	CdSe
	E_{g_0} [eV]	1.42	2.16
	E_{g_1} [eV]	4.93	7.43
	E_{P_0} [eV]	24.69	17.52
	E_{P_1} [eV]	1.05	0.79
	E_{P_2} [eV]	13.49	13.24
	m_c^*/m_0	0.056	0.114
[001]	m_{lh}^*/m_0	0.056	0.118
[111]	m_{lh}^*/m_0	0.047	0.098
[001]	m_{hh}^*/m_0	0.334	0.597
[111]	m_{hh}^*/m_0	0.776	1.241
[001]	γ_1	10.39	5.07
[111]	γ_1	11.22	5.51
	γ_2	3.70	1.69
	γ_3	4.97	2.35

Table 1: Calculated parameters for 8 and 14 $\mathbf{k} \cdot \mathbf{p}$ Hamiltonians, for GaAs and CdSe ZB lattices obtained with B3LYP functional.

Effective masses are defined by the curvature of the band dispersion at high symmetry points in the IBZ, in this case Γ :

$$\left(\frac{1}{m^*} \right)_{\mu\nu} = \frac{1}{\hbar^2} \frac{\partial^2 E_k}{\partial k_\mu \partial k_\nu} \quad (3)$$

An alternative definition of the effective mass, from $\mathbf{k}\cdot\mathbf{p}$ theory, depends on the interaction between bands around the conduction and valence band edges, where i is the band for which the effective mass is being calculated:

$$\frac{1}{m_i^*} = \frac{1}{m_0} + \frac{2}{m_0} \sum_{i \neq j} \frac{|p_{ij}|^2}{|E_i - E_j|} \quad (4)$$

The effective mass calculated using this expression can be systematically improved by considering additional interactions from remote bands. For the methodology to be consistent, convergence of the two should be observed as further bands are considered in Eq. 4. Indeed, this is observed, as shown in Table 2. We use shortened notation: $p_0 = p_{\Gamma_{1c}, \Gamma_{5v}}$, $p_1 = p_{\Gamma_{5c}, \Gamma_{1c}}$, $p_2 = p_{\Gamma_{5c}, \Gamma_{5v}}$.

	Eq. (3)	Eq. (4)		
		p_0	p_0, p_1	p_0, p_1, p_2
GaAs	0.0561	0.0552	0.0561	0.0561

Table 2: Convergence of calculated effective mass at the conduction band edge of GaAs as additional band couplings, p_i , taken into account.

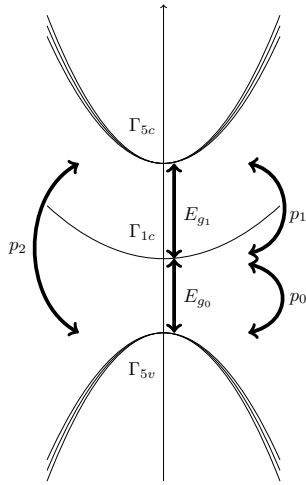


Figure 1: Schematic of ZB band structure around Γ point. Top of valence band, Γ_{5v} , bottom of conduction band, Γ_{1c} , and second conduction band, Γ_{5c} . Energy gaps, E_{q_i} , and coupling parameters, p_i , correspond to the notation in table 1.

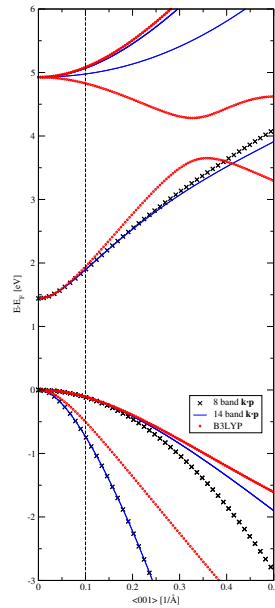


Figure 2: Band structure of GaAs along $[001]$ direction in the IBZ, obtained by DFT-B3LYP (open circles), 8 band $\mathbf{k}\cdot\mathbf{p}$ Hamiltonian (crosses), and 14 band $\mathbf{k}\cdot\mathbf{p}$ Hamiltonian (lines).

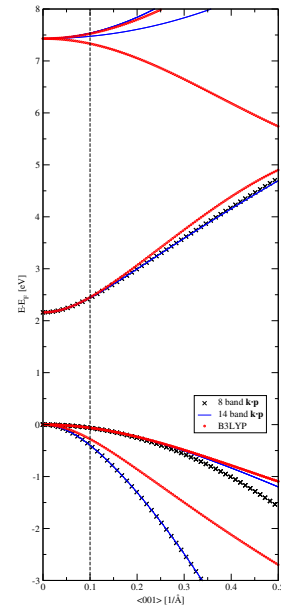


Figure 3: Band structure of CdSe along $[001]$ direction in the IBZ, obtained by DFT-B3LYP (open circles), 8 band $\mathbf{k}\cdot\mathbf{p}$ Hamiltonian (crosses), and 14 band $\mathbf{k}\cdot\mathbf{p}$ Hamiltonian (lines).

The Luttinger parameters relate to the valence band edge effective masses along directions of high symmetry in the IBZ and largely determine the band curvature. They are calculated from appropriate pairs of the following system of equations, along different high symmetry directions:

$$\begin{aligned} \left(\frac{m_0}{m_{hh}^*}\right)^{[001]} &= \gamma_1 - 2\gamma_2, & \left(\frac{m_0}{m_{hh}^*}\right)^{[110]} &= \frac{1}{2}(2\gamma_1 - \gamma_2 - 3\gamma_3), & \left(\frac{m_0}{m_{hh}^*}\right)^{[111]} &= \gamma_1 - 2\gamma_3, \\ \left(\frac{m_0}{m_{lh}^*}\right)^{[001]} &= \gamma_1 + 2\gamma_2, & \left(\frac{m_0}{m_{lh}^*}\right)^{[110]} &= \frac{1}{2}(2\gamma_1 + \gamma_2 + 3\gamma_3), & \left(\frac{m_0}{m_{lh}^*}\right)^{[111]} &= \gamma_1 + 2\gamma_3, \end{aligned} \quad (5)$$

As the effective mass tensors are anisotropic, we obtain different Luttinger parameters along each direction, as detailed in table 1.

Fig. 1 depicts the schematic band structure of the ZB structure, taken into account by the 14 band $\mathbf{k}\cdot\mathbf{p}$ Hamiltonian. The 8 band Hamiltonian (C_{4v}) includes only the Γ_{5v} valence and Γ_{1c} conduction bands, coupled by the p_0 dipole interaction. The p_1 interaction is isomorphic with p_0 , however the inclusion of the p_2 interaction between Γ_{5v} and Γ_{5c} bands has the effect of reducing the symmetry to C_{2v} , as required to resemble the correct atomistic structure of ZB lattice.

Figs. 2 and 3 show the band structures along the $\langle 001 \rangle$ direction in the IBZ for GaAs and CdSe, respectively. Largely good agreement between the DFT and $\mathbf{k}\cdot\mathbf{p}$ calculations is seen up to 0.1 \AA^{-1} . In addition to observing the correct C_{2v} symmetry, the 14 band model shows a notable improvement in its depiction of the heavy hole band well beyond this region. Of greatest note is the inclusion of the higher conduction bands in the 14 band model.

4. Conclusion

We have demonstrated that the use of hybrid functionals in DFT calculations can be used to effectively and accurately parameterise multiband $\mathbf{k}\cdot\mathbf{p}$ Hamiltonians for some common ZB semiconductors. Further, we have shown that the 14 band model, by inclusion of higher conduction bands and having the correct C_{2v} symmetry of the ZB lattice, affords greater accuracy in the prediction of the band structure than the more widely used 8 band model, which is typically synonymous with $\mathbf{k}\cdot\mathbf{p}$ perturbation theory.

Acknowledgments

The authors acknowledge the EPSRC for the grant ‘‘Enhanced multiple exciton generation in colloidal quantum dots.’’ The authors also thanks Leonardo Bernasconi, Jacek Miloszewski, and Nenad Vukmirović for useful discussions. Mark Lundie acknowledges the University of Salford for the award of Graduate Teaching Studentship.

References

- [1] Christensen N E 1984 *Phys. Rev. B* **30** 5753
- [2] Rideau D, Feraille M, Ciampolini L, Minondo M, Tavernier C and Jaouen H 2005 *Phys. Rev. B* **74** 195208
- [3] Heyd J, Peralta J E, Scuseria G E and Martin R L 2005 *J. Chem. Phys.* **123** 174101
- [4] Tomić S, Montanari B and Harrison N M 2008 *Physica E* **40**
- [5] Tomić S and Vukmirović N 2011 *J. Appl. Phys.* **110** 053710
- [6] Dovesi R, Saunders V R, Roetti C, Orlando R, Zicovich-Wilson C, Pascale F, Civalleri B, Doll K, Harrison N M, Bush I J, D’Arco P and Llunell M 2009 *CRYSTAL 09 Manual*
- [7] Bush I J, Tomić S, Searle B G, Mallia G, Bailey C L, Montanari B, Bernasconi L and Harrison N M 2011 *Proceedings of the Royal Society A* **467** 2112
- [8] Perdew J P, Ernzerhof M and Burke K 1996 *J. Chem. Phys.* **105** 9982–9985
- [9] Becke A D 1993 *J. Chem. Phys.* **98** 1372–1377
- [10] Monkhorst H J and Pack J D 1976 *Phys. Rev. B* **13**(12) 5188–5192
- [11] Tomić S, Sunderland A G and Bush I J 2006 *J. Mater. Chem.* **16**(20) 1963–1972